Development of PtGe and PtIn anodic catalysts supported on carbonaceous materials for DMFC

CrossMark

Natalia S. Veizaga [a,*], Valdecir A. Paganin [b], Thairo A. Rocha [b], Osvaldo A. Scelza [a], Sergio R. de Miguel [a], Ernesto R. Gonzalez [b]

[a] Instituto de Investigaciones en Catálisis y Petroquímica "Ing. José M. Parera" (INCAPE), Facultad de Ingeniería Química (UNL) − CONICET, Santiago del Estero 2654, 3000 Santa Fe, Argentina
[b] Instituto de Química de São Carlos, USP, C.P.780, São Carlos, SP 13560-970, Brazil

ARTICLE INFO

ABSTRACT

Bimetallic PtGe and PtIn catalysts (Ge/Pt and In/Pt molar ratios = 0.33, 17 wt.% Pt loading) were prepared over carbonaceous supports (carbon Vulcan, carbon nanotubes and structured mesoporous carbon). The liquid phase deposition−reduction method by using 0.4 M sodium borohydride as a reducing agent was employed. The electrocatalytic activity for methanol oxidation was compared with a commercial Pt/CV E-TEK catalyst. The onset potential of the CO oxidation was shifted to less positive values for carbon Vulcan and carbon nanotubes supported catalysts and with a smaller effect in the case of mesoporous carbon supported ones. The best electrocatalytic performance was obtained by using carbon Vulcan as support of bimetallic catalysts, followed by carbon nanotubes. The performance of mesoporous carbon as a support was not adequate. PtGe/CV, PtGe/NT and PtIn/CV catalysts displayed the best performance in DMFC. The good performance of these catalysts could be due to the presence of small particle sizes with a narrow distribution, and to geometric effects (observed from different characterization techniques) related to a probable decoration of Ge or In around the small Pt particles.

1. Introduction

The objective of producing new and more efficient electrocatalysts is a very important goal in the development of low temperature fuel cells, mainly in the named direct conversion cells, which use organic molecules such as methanol, ethanol and formic acid. Direct methanol fuel cells (DMFC) are promising systems for energy conversion due to the high efficiency, low emission of contaminants and low operation temperatures [1,2]. Important efforts have been made in order to develop an adequate technology for the DMFC, mainly in the field of the development of very active catalysts for the electro-oxidation of methanol. Electrochemical studies show that CO, formic acid and formaldehyde are the intermediary compounds in the oxidation of methanol on Pt electrodes [3,4]. The electro-oxidation of methanol over Pt involves several intermediate steps such as dehydrogenation, CO chemisorption, adsorption of OH (or H_2O), chemical reaction between adsorbed CO and OH, and evolution of CO_2. One of them is the limiting step which depends on the temperature and the characteristics of the catalytic surface (crystallographic

orientation, presence of defects) [5]. The electro-oxidation reactions of organic compounds of low molecular weight (methanol, ethanol, formaldehyde, formic acid) require a catalyst containing a noble metal like Pt. However, all these reactions produce CO, which is strongly adsorbed on Pt. Hence an important number of works try to modify the vicinity of Pt atoms by adding other elements [5].

One of the roles of the added elements to Pt/C is to facilitate the CO oxidation on the catalyst surface via a bifunctional mechanism or by a ligand effect or a combination of both effects. The bifunctional mechanism enhances the catalytic oxidation of CO through the presence of oxyhydride species dispersed on the catalytic surface. The effect of these groups is the diminution of the CO oxidation potential. Moreover, the addition of a second element modifies the water and oxygen adsorption properties [6].

Presently, PtRu catalysts have been extensively studied as anodic electrocatalysts for DMFC, since Pt is the responsible of the methanol activation to produce CO, while Ru is the responsible for the CO conversion into CO_2 [7].

Several authors studied PtRu catalysts with both metals forming alloys and these catalysts were compared with others which do not form alloys between Pt and Ru [5,8]. They observed that both catalyst types were active for the methanol oxidation, but the catalysts with the smaller amount of RuO_x, which display the smaller Ru–O bond energy (Pt–Ru alloys), showed the best results. In addition, the electrocatalysts for DMFC based on PtRu presented a higher activity than Pt alone or Pt doped with other metals. The state of Ru in these catalysts is under discussion up to now, since the alloy degree between Pt and Ru and the content of RuO_xH_y are the main factors to define the catalytic activity. Though for some authors, the catalyst containing Pt–RuO_x species is slightly more active than that with alloyed PtRu species, the last one appears to have a better stability [9]. Dubau et al. [10] reported that Ru appears to decorate the Pt, and presents a better tolerance to CO than the Pt–Ru alloys with the same Pt/Ru atomic ratio. Neto et al. [11] made a comparison of PtSn/C, PtRu/C and PtSnRu/C catalysts prepared by the ethylenglicol method for methanol and ethanol oxidations. The XRD spectra showed that PtRu/C catalyst displayed a fcc structure, typical of the alloyed Pt with Ru, while PtSn/C and PtSnRu/C catalysts showed not only alloyed compounds but also the presence of SnO_2 phase. By using amperometric measurements it was found that the PtSn/C catalysts were more active than PtRu/C and PtSnRu/C for the oxidation of methanol and ethanol at room temperature. The higher yield of the PtSn/C catalyst could be due to the fact that a fraction of Sn would be forming alloys with Pt, thus modifying the electronic properties of Pt. Hence, in this way the capacity of the metallic surface to adsorb methanol and ethanol and to dissociate the C–H bond is modified. Besides, it was found that SnO_2 species enhance the oxidation of the adsorbed oxidized intermediary (bifunctional mechanism).

With respect to the PtGe couple for fuel cells, few papers have been reported in the literature. Crabb et al. [12] found that when the catalyst was prepared by controlled surface reaction, there was a promotional effect of GeO_2 at low potentials, though this effect was not very important and it does not change with the Ge loading. By using CO stripping measurements on PtGe catalysts, it was observed a diminution of

the total amount of CO, thus indicating that the Pt sites could be covered by Ge. In addition, the combination of Pt with Ge appears to have an incidence on the adsorption properties of CO on the Pt surface. With respect to PtIn couple for fuel cells, the literature only mentions one work about PtSnIn catalysts [13], finding a promoter effect of In on the ethanol electro-oxidation activity.

The development of more efficient electrocatalysts with lower affinity to CO is a very important point in order to achieve technological advances in DMFC. In conclusion, an ideal anodic catalyst would be such that it must be completely tolerant to CO, thus reaching a total oxidation of CO to CO_2 at very low potentials.

In this paper two few studied bimetallic systems are proposed: PtGe and PtIn supported on different carbonaceous materials (carbon Vulcan, carbon nanotubes and mesoporous carbon) which were compared with a commercial Pt/VC E-TEK catalyst. Taking into account that there is little information in the literature about these bimetallic couples in fuel cells, and that this literature reported that both Ge and In could be promising systems, the objective of this paper is the development of PtGe and PtIn anodic catalysts supported on carbonaceous materials to be used in direct methanol fuel cells. The proposed systems were characterized by temperature programmed reduction (TPR), H_2 chemisorption, benzene hydrogenation, X-ray diffraction (XRD), X-ray photoelectron spectroscopy (XPS), CO stripping and transmission electron microscopy (TEM). Moreover, a laboratory cell (DMFC) was used for testing the catalysts under different temperature and pressure conditions.

2. Experimental

2.1. Preparation of the electrocatalysts

Electrocatalysts based on supported PtGe and PtIn were prepared by a deposition–reduction in liquid phase method, by using sodium borohydride 0.4 M (RB) as a reductive agent. The catalysts contained 17 wt.% Pt and the second metal were added maintaining a Ge/Pt or In/Pt molar ratio of 0.33. The metallic precursors were H_2PtCl_6, $GeCl_4$ and $In(NO_3)_3$. Three different supports were used: carbon Vulcan XC-72 (CV), multiwall carbon nanotubes (NT) and a structured mesoporous carbon from CNEA-Argentina (MC). Vulcan carbon XC-72 has a specific surface area (S_{BET}) of 240 $m^2 g^{-1}$, a pore volume (V_{pore}) of 0.31 $cm^3 g^{-1}$ and a mean particle size of 40 nm. Commercial multiwall carbon nanotubes (MWCN from Sunnano, purity >90%, diameter: 10–30 nm, length: 1–10 μm) with the following textural properties: $S_{BET} = 211 m^2 g^{-1}$, $V_{pore} = 0.46 cm^3 g^{-1}$, were used. The physical properties of the structured mesoporous carbon, were: $S_{BET} = 476 m^2 g^{-1}$, $V_{pore} = 0.35 cm^3 g^{-1}$. A maximum in the pore size distribution is found at around 9 nm. The micro- (<2 nm) and meso-porosity (between 2 and 50 nm) is attributed to the structure of the carbon, which consists of clusters of porous uniform spheres in a fairly regular array. Therefore, the obtained material has a hierarchical pore structure (micro- and meso-porosity) [14,15].

The liquid phase deposition–reduction was carried out at 50–60 °C. When the basic solution $NaBH_4$ 0.4 M was added in

several steps, the reduction begins at an acid pH and finishes at a basic pH. An aqueous H_2PtCl_6 solution of 30 gPt L^{-1} and a $NaBH_4$ 0.4 mol L^{-1} in 1 mol L^{-1} NaOH solution were prepared. For the metal deposition, the carbon particles were wetted with a solvent of low surface tension, such as absolute ethanol (10 mL g support^{-1}), in order to enhance the metal deposition on a carbon of high surface area. Then a mixture of the corresponding metallic precursors (Pt to obtain 17 wt.% and Ge to obtain 2.45 wt.% or In to obtain 3.88 wt.%; molar ratio = 0.33) was added to the wetted carbon support. The metallic addition was carried out dropping the solutions of the metallic precursors under continuous stirring. This suspension was maintained under stirring during 30 min at 60 °C to favour the homogeneous deposition of the metals on the support. After this period, the reductive agent ($NaBH_4$) was added in four steps (30 min) in a ratio of 6.4 mL g^{-1} C. The catalysts were finally filtered, washed with distilled water and dried in vacuum at 70 °C for 3 h [16].

2.2. Characterization of the electrocatalysts

2.2.1. Temperature programmed reduction

After deposition of the metals, catalysts previously dried under vacuum at 60 °C were reduced by using a reductive mixture (10 mL min^{-1} of H_2 (5%v/v)-N_2 in a flow reactor. Samples were heated at 6 °C min^{-1} from 25 °C to 800 °C. The exit of the reactor was connected to a TCD in order to obtain the TPR signal.

2.2.2. X-ray photoelectron spectroscopy (XPS)

XPS measurements were carried out in a Multitechnic Specs Photoemission Electron Spectrometer equipped with an X-ray source Mg/Al and a hemispherical analyser PHOIBOS 150 in the fixed analyser transmission (FAT) mode. The spectrometer operates with an energy power of 100 eV and the spectra were obtained with a pass energy of 30 eV and a Mg anode operated at 90 W. The analysis chamber was kept at pressure lower than 1.5×10^{-8} torr. The binding energies (BEs) of the signals were referred to the C1s peak at 284 eV. Peak areas values were estimated by fitting the signals with a combination of Lorentzian–Gaussian curves of variable proportion and using the CasaXPS Peak fit software version 1.

2.2.3. H_2 chemisorption

The H_2 chemisorption measurements were made in a volumetric equipment at room temperature. The sample weight used on the experiments was 0.100 g, this being previously outgassed under vacuum (10^{-4} torr) at room temperature. The H_2 adsorption isotherms were obtained at room temperature between 25 and 100 torr. The isotherms were linear in the range of used pressures and the H_2 chemisorption capacities were calculated by extrapolation of the isotherms to zero pressure [17].

2.2.4. X-ray diffraction

The XRD experiments were carried out at room temperature in a spectrometer Shimadzu model XD3A by using radiation CuKα (λ = 1.542 Å) at 30 kV and a current of 40 mA, being the scanning range between 20 and 100°.

2.2.5. CO stripping

Catalysts were characterized by means of CO stripping (electrochemical characterization) in a conventional cell with three electrodes, using a potentostat/galvanostat (TEQ-02, Argentina). Pure CO is bubbled in an electrolytic solution of H_2SO_4 0.5 M. CO is quickly adsorbed on the Pt surface producing a CO adsorbed monolayer. During the CO adsorption process (1 h), the potential of the cell is maintained constant at 200 mV (this value is lower than the CO oxidation potential). Then an inert gas (N_2 or Ar) is passed to purge the electrolytic solution in order to eliminate the dissolved CO, thus remaining only the adsorbed CO on the Pt surface. In these conditions, and maintaining constant the flow of inert gas, the potential was modified in order to induce the CO oxidation. When the Pt surface is covered by a monolayer of CO, the hydrogen adsorption is inhibited. Hence the typical H_2 adsorption and desorption peaks do not appear in the cyclic voltammograms. When the CO monolayer is removed by oxidation at high potentials, the Pt surface is able to adsorb and desorb H_2, thus appearing the corresponding peaks. In order to observe the process of occupation and releasing of the Pt active sites by CO, the potentials of the voltammetry are programmed so that the potential starts at open circuit under N_2 atmosphere and it is cycled between −200 and 1200 mV (vs. Ag/AgCl). In this way in the first cycle, the H_2 adsorption–desorption characteristic peaks are not detected and at higher potentials the CO stripping peak is produced by oxidation of CO to CO_2 which is released from the Pt surface. In the second cycle the characteristic peaks of H_2 are clearly observed and they correspond to those observed in a conventional voltammetry of a Pt electrode in contact with H_2.

The specific electrochemical active area (EASS) Eq. (1) is an important parameter for the comparison of the electroactivity of the catalysts. This parameter is obtained from the CO voltammetry (CO desorption peak) as:

$$EASS = \frac{(Q_{CO}/q_{CO}^s)}{m_{Pt}} \qquad (1)$$

where m_{Pt} is the Pt mass, Q_{CO} is the charge required for the oxidation of the monolayer of CO adsorbed on the active sites, and q_{CO}^s is a reference value equal to 0.42 mC cm^{-2} (assuming that the surface density of polycrystalline Pt is $1.3 \cdot 10^{15}$ atoms cm^2, that each CO molecule is adsorbed on a single Pt atom, and that two electrons are involved in the oxidation of CO to CO_2 [18]).

2.2.6. Benzene hydrogenation reaction

The test reaction of the metallic phase (benzene hydrogenation -Bz-) was carried out in a differential flow reactor at 110 °C. In this case a molar ratio H_2/Bz = 26 and a volumetric rate of 600 mL min^{-1} were used. The sample weight was such as to obtain a conversion lower than 5% (10–20 mg). The reaction products were analysed by using a gas chromatographic system (packed column with Chromosorb and FID as detector).

2.2.7. Transmission electron microscopy (TEM)

Transmission electron microscopy (TEM) measurements were carried out on a JEOL 100CX microscope, operated with an

acceleration voltage of 100 kV, and magnification ranges of 80,000× and 100,000×. For each catalyst, a very important number of Pt particles (approximately 200) were observed and the distribution of particle sizes was done on this basis. The mean particle diameter (d) was calculated as: $d = \Sigma(ni \cdot d_i)/\Sigma ni$; where ni is the number of particles of diameter d_i.

2.2.8. Tests in a DMFC cell

All electrodes were made to contain 1 mg Pt cm^{-2}. A commercial Pt/CV E-TEK 30 wt.% was used in the cathode, while the bimetallic PtGe and PtIn catalysts prepared by deposition–reduction in liquid phase were used in the anode. The experiments in the DMFC were carried out at 70 and 90 °C, using O$_2$ saturated in water in two conditions: at 70 °C and atmospheric pressure, and 90 °C and 2 atm. The geometric area of the electrodes was 4.62 cm^{-2}. In all cases, a Nafion 115 membrane was used as electrolyte. The membrane and electrode assemblies (MEAs) were prepared by hot-pressing two electrodes on both sides of a pre-treated Nafion® 115 membrane (H$^+$, DuPont) at 125 °C and 5 MPa for 2 min. The MEA was placed between two high-density carbon plates in which serpentine-type channels were machined for the circulation of O$_2$ (70 mL min^{-1}) and a methanol solution (2 mol L^{-1}).

3. Results and discussion

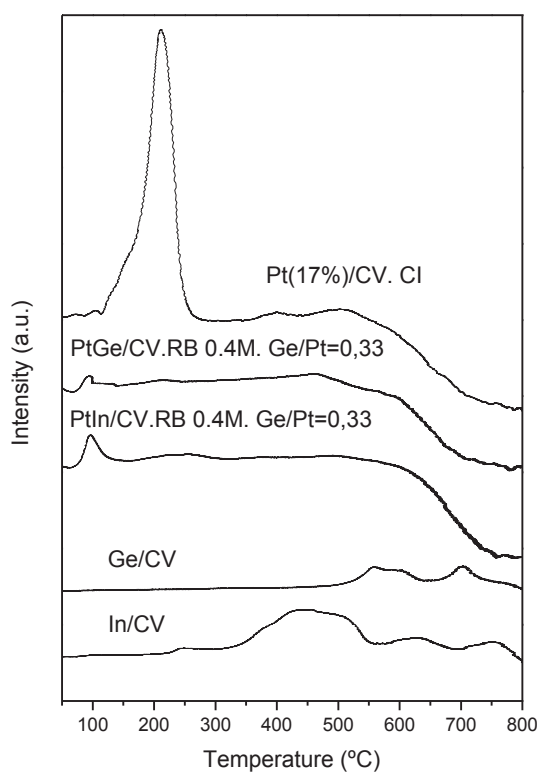The TPR profiles were determined on the different catalysts prepared by deposition–reduction in liquid phase of both

Table 1 – H$_2$ chemisorption capacity and crystallite diameter obtained by XRD (d_{XRD}) for the different samples supported on the three carbonaceous materials.

Catalysts	H$_2$ chemisorption capacity (μmol H$_2$/g cat)	d_{XRD} (nm)
Pt/CV. RB 0.4 M	138	6
PtGe/CV. RB 0.4 M	214	4.4
PtIn/CV. RB 0.4 M	166	4.3
Pt/NT. RB 0.4 M	83	6
PtGe/NT. RB 0.4 M	184	–
PtIn/NT. RB 0.4 M	180	4.9
Pt/MC. RB 0.4 M	212	5
PtGe/MC. RB 0.4 M	169	5.8
PtIn/MC. RB 0.4 M	123	8.4

metallic precursors. Fig. 1 shows a comparison of the profiles of PtGe and PtIn bimetallic catalysts supported on CV with the TPR profiles of In/CV and Ge/CV prepared in the same way, and the profile of Pt/CV prepared by conventional impregnation. It can be observed in Fig. 1 that Pt/CV prepared by conventional impregnation (CI) presents a well defined peak at 210–220 °C (maximum of the peak). This peak corresponds to the reduction of Pt oxychlorides, in agreement with other results obtained on Pt catalysts supported on different carbonaceous materials [19]. The Ge/CV and In/CV monometallic catalysts show reduction temperatures higher than 300 °C, being the Ge reduction more difficult than the In one. The TPR profiles of PtGe and PtIn supported on carbon Vulcan and prepared by deposition–reduction in liquid phase with sodium borohydride do not show any important reduction peak in the temperature zone where Pt is reduced in the impregnated catalysts. Besides, there are no important peaks at higher temperatures. These results would indicate that after the deposition–reduction in liquid phase, the main fraction of Pt would be as Pt(0). It must be noted that from these results it was not possible to obtain information about the Ge and In reducibility degree. Besides, similar TPR results were obtained for the PtGe and PtIn bimetallic samples supported on the other carbonaceous materials (NT and MC).

In order to obtain information about the reducibility of the different metallic species, the bimetallic PtGe and PtIn catalysts were analysed by XPS. From the deconvolution of the spectra on all the supports used in the catalysts preparation, it was obtained one peak at 71.8 eV for Pt 4f$_{7/2}$ and another one at 74.6–75.0 eV for Pt 4f$_{5/2}$. These peaks can be assigned to zerovalent Pt. Besides, other small doublets are present at 75.2 eV and 78.0–78.4 eV, which correspond to Pt oxides or oxychlorides [20]. The concentrations of surface Pt oxidized species are lower than 35% of the total Pt species. This means that the major fraction of surface Pt is in metallic state for catalysts supported on the different supports. The presence of surface Pt oxidized species could be due to a surface oxidation process during the storage of the samples previous to XPS determinations. With respect to the oxidation state of the promoters in the bimetallic catalysts, XPS results for Ge 3d showed that all surface Ge is in an oxidized state in all PtGe catalysts, while for bimetallic catalysts containing In, XPS results showed the presence of both oxidized In species and zerovalent In species.

Fig. 1 – TPR profiles of catalysts supported on CV prepared by reduction with sodium borohydride (RB) and conventional impregnation (CI).
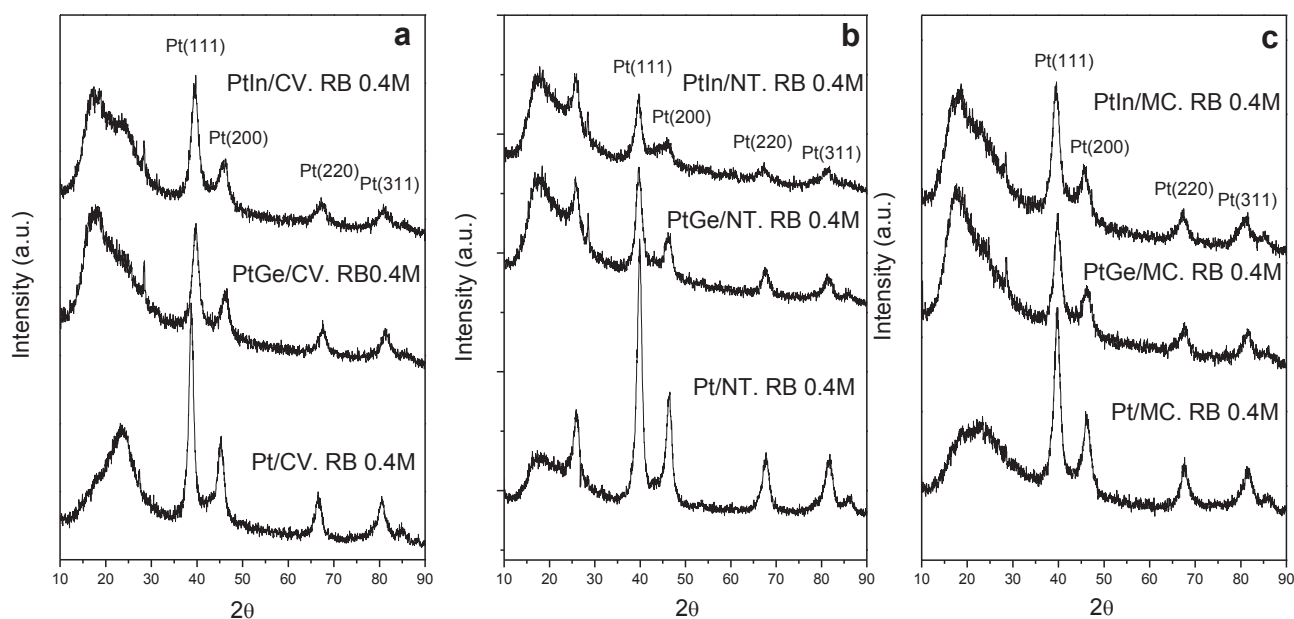
Fig. 2 – XRD results for different bimetallic catalysts supported on the different carbonaceous materials. a) supported on CV, b) supported on NT and c) supported on MC.

Table 1 shows the H_2 chemisorption capacity of the different samples supported on the different carbonaceous materials. It must be noted that the bimetallic catalysts supported on CV and NT display a higher chemisorption capacity than the corresponding monometallic ones. On the other hand the bimetallic catalysts supported on MC show an inverse behaviour. These different behaviours with respect to the H_2 chemisorption capacity according to the nature of the support can be explained by a different structure of the metallic phase as a function of the support, as it will be discussed below.

Fig. 2a), b) and c) shows the XRD results for the different bimetallic catalysts. In all cases, the diffractograms indicate the presence of fcc structures, typical of the metallic Pt, represented by (111), (200), (220) and (311) planes, which appear at 2θ values of 39.8°, 46.3°, 67.5° and 81.6°, respectively. The broadening of the XRD peaks is indicative of the crystallite size. Table 1 displays the results of crystallite sizes obtained by using Scherrer equation [21] applied to the (111) plane. It is observed that PtGe and PtIn catalysts supported both on CV and NT show a slightly smaller crystallite sizes with respect to the corresponding monometallic Pt, while bimetallic catalysts supported on MC display higher sizes than the corresponding monometallic Pt one.

The XRD crystallite sizes are in agreement with the H_2 chemisorption values, which indicate that the chemisorption values increase for the bimetallic catalysts supported on CV and NT (with respect to that of the corresponding monometallic material). Such as it was previously mentioned, the behaviour of the bimetallic catalysts supported on MC is the opposite. These results indicate a strong influence of the support on the characteristics of the metallic phase.

Benzene hydrogenation is a structure-insensitive reaction, which can be carried out on one active metallic site [22,23]. In

consequence, the values of the initial rate (R^0_{Bz}) could be related with the amount of exposed surface active sites. Likewise, the changes in the activation energies (Ea_{Bz}) can be related to electronic modifications of the active sites. This test reaction of the metallic phase can be used for the characterization of catalysts prepared by deposition–reduction in liquid phase at low temperature, since the temperature used for this reaction is also low, and in these conditions there are no changes in the characteristics of the catalysts by the temperature. Table 2 shows the results of activation energies in benzene hydrogenation (Ea_{Bz}) for the different mono and bimetallic catalysts and the values of initial reaction rates (R^0_{Bz}). It can be observed that there are slight modifications of the initial rate when the second metal, either Ge or In, is added to Pt. However, the R^0_{Bz} values of the bimetallic catalysts supported on CV and NT are higher than the value of the corresponding monometallic catalyst, which agree with chemisorption and XRD results. Results show that no important blocking or dilution effects of both promoters on Pt would be present on the metallic phase, since both the hydrogen

Table 2 – Activation energies (Ea_{Bz}) and initial reaction rates (R^0_{Bz}) in benzene hydrogenation at 110 °C for different catalysts.

Catalysts	Ea_{BZ} (Kcal/mol)	R^0_{Bz} (mol/h g Pt)
Pt/CV. RB 0.4 M	10.1	2.6
PtGe/CV. RB 0.4 M	—	—
PtIn/CV. RB 0.4 M	12.2	3.9
Pt/NT. RB 0.4 M	13.5	3.9
PtGe/NT. RB 0.4 M	16.8	5.2
PtIn/NT. RB 0.4 M	12.1	4.1
Pt/MC. RB 0.4 M	12.3	3.7
PtGe/MC. RB 0.4 M	9.8	1.3
PtIn/MC. RB 0.4 M	13.0	3.7

chemisorption and R^0_{Bz} values do not decrease with the second metal addition. Besides, the activation energy is slightly modified by the addition of the second metal to Pt in all the supports, thus indicating low electronic interactions between Pt and the second metal, Ge or In. Hence, these results would indicate that only geometric effects related with a probable decoration of Ge and In around the small Pt particles could be present in the bimetallic catalysts supported on CV and NT.

Fig. 3 shows the cyclic voltammograms of CO stripping corresponding to Pt, PtGe and PtIn catalysts supported on the different carbonaceous materials. When the metallic surface

is covered by a CO monolayer, the atomic H electroadsorption is inhibited and the peak due to the oxidation of CO into CO_2 is produced at a given potential. The Pt/CV catalyst shows a main CO oxidation peak at about 0.51 V vs. Ag/AgCl. This value is very close to that obtained by Vidakovic et al. [24] for non supported Pt (0.536 V).

In both bimetallic catalysts (PtGe and PtIn) supported on CV, the CO oxidation peak is divided. A main peak appears at similar potentials than in the monometallic materials, which can be due to the oxidation of strongly adsorbed CO on the metallic sites. Besides, a small peak at 0.40 V vs. Ag/AgCl is
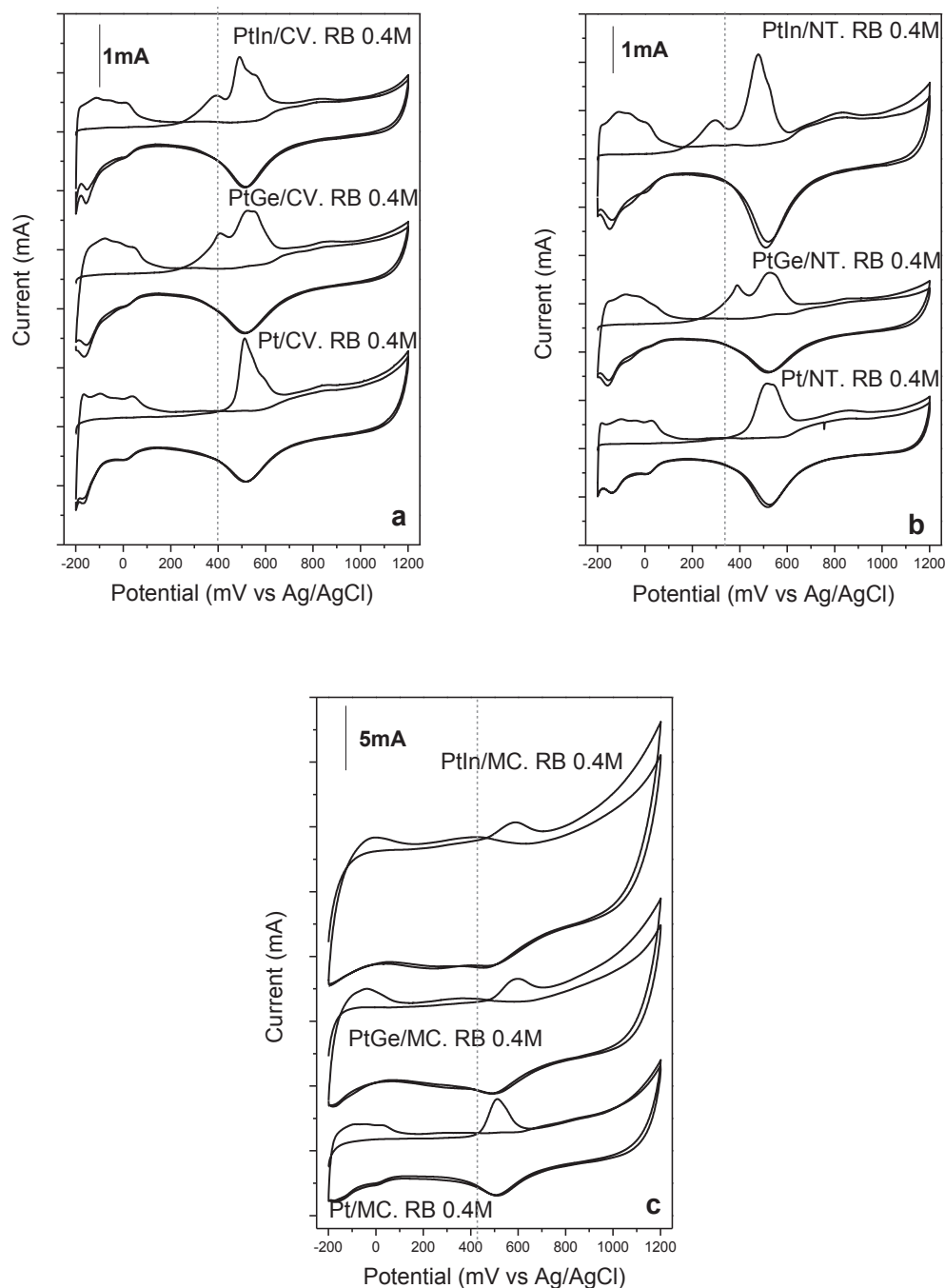

Fig. 3 − Cyclic voltammograms of CO stripping corresponding to Pt, PtGe and PtIn catalysts supported on the different carbonaceous materials a) supported on CV, b) supported on NT and c) supported on MC.

Table 3 – Electrochemically active specific surface (EASS) obtained from CO stripping voltammetry for different catalysts.

Catalysts	EASS (m^2/g Pt)
Pt/CV. RB 0.4 M	12
PtGe/CV. RB 0.4 M	20
PtIn/CV. RB 0.4 M	18
Pt/NT. RB 0.4 M	31
PtGe/NT. RB 0.4 M	20
PtIn/NT. RB 0.4 M	28
Pt/MC. RB 0.4 M	48
PtGe/MC. RB 0.4 M	27
PtIn/MC. RB 0.4 M	25

monometallic catalyst is positioned at 0.40 V vs. Ag/AgCl. From these results it is observed a promotion effect of both Ge and In, which facilitates the CO oxidation at lower potentials. A similar Ge promotion effect on Pt was also observed by Crabb y Ravikumar [12].

Similar effects, though with small differences in the behaviour of the catalysts supported on CV, were observed for the catalyst supported on NT. Thus for the monometallic Pt/NT catalyst, the onset potential is placed at 0.35 V, whereas such potential is shifted to lower potentials in bimetallic ones (0.22 V for PtGe/NT and 0.16 V for PtIn/NT). With respect to the maximum of the oxidation peak for Pt/NT, it was observed a broad peak with a maximum between 0.51 and 0.54 V vs. Ag/AgCl. Furthermore, both bimetallic catalysts supported on NT show a main oxidation peak similar to that of the corresponding monometallic one (0.53 V and 0.48 V for PtGe and PtIn, respectively), and a small peak at lower potential (0.39 and 0.29 V vs. Ag/AgCl for PtGe and PtIn, respectively). Hence, in these cases it is also observed a promotion effect of Ge and In on Pt.

also observed, which can be attributed to the CO oxidation of species weakly adsorbed on other metallic sites probably modified by the presence of the second metal in the vicinity of Pt. Moreover, it can be also observed in both bimetallic catalysts that the potential of the beginning of the oxidation (onset potential) is placed at 0.22 V, while that corresponding to the
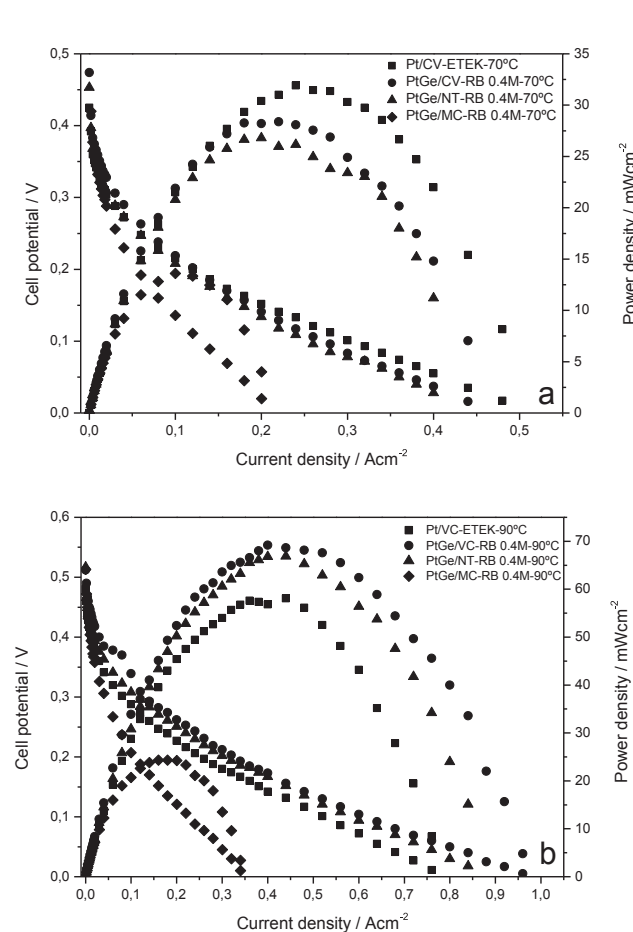

Fig. 4 – Polarization curves and power density curves in single DMFC with PtGe/CV, PtGe/NT and PtGe/MC prepared by RB as anode electrocatalysts and commercial Pt/CV (E-TEK) as cathode for methanol oxidation at a) 70 °C and 1 atm O_2 pressure, b) 90 °C and 2 atm O_2 pressure, using a 2 mol L^{-1} methanol solution. Anode metal loading 1 mg cm^{-2}. Cathode 30 wt.% Pt/CV, Pt loading 1 mg cm^{-2}.
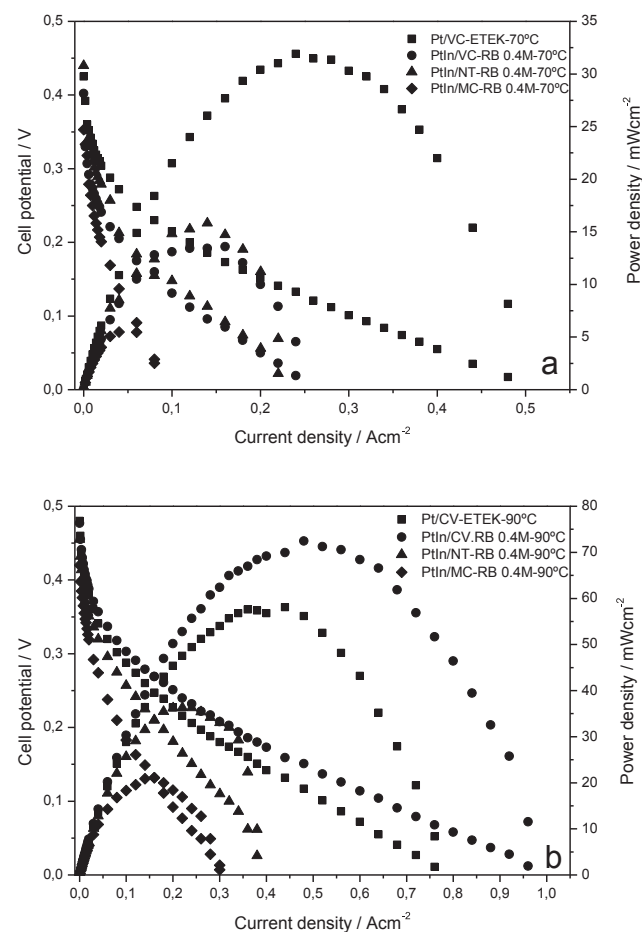
Fig. 5 – Polarization curves and power density curves in single DMFC with PtIn/CV, PtIn/NT and PtIn/MC prepared by RB as anode electrocatalysts and commercial Pt/CV (E-TEK) as cathode for methanol oxidation at a) 70 °C and 1 atm O_2 pressure, b) 90 °C and 2 atm O_2 pressure, using a 2 mol L^{-1} methanol solution. Anode metal loading 1 mg cm^{-2}. Cathode 30 wt.% Pt/CV, Pt loading 1 mg cm^{-2}.

The behaviour of the bimetallic catalysts supported on MC is opposite to that of those supported on CV and NT. By analysing the behaviour of the catalysts supported on MC, it was found a main CO oxidation peak at 0.52 V for the monometallic sample and at 0.58 V for the bimetallic PtGe/MC and PtIn/MC, while the onset potential is 0.42 V for the monometallic one and 0.47 V for the bimetallic samples. The shift of the onset potential to higher values indicates a more difficult CO oxidation on these bimetallic catalysts than on the monometallic one. One main difference is observed with respect to the catalysts supported on CV and NT, there are no oxidation peaks at lower potentials, which indicates that there are no promotion effects of Ge and In on Pt for this

support. This behaviour could be explained by the high resistivity of the mesoporous carbon, as it was reported by Vengatesan et al. [25]. With reference to the EASS values reported in Table 3, obtained from the CO stripping experiments, it can be observed that only the bimetallic catalyst supported on CV showed higher values with respect to the corresponding monometallic one, while those bimetallic samples supported on NT had similar values than the corresponding monometallic one. The bimetallic catalysts supported on MC showed lower areas than the corresponding to the monometallic sample.

Fig. 4a) and b) shows the polarization and power density curves obtained in a direct methanol fuel cell (DMFC) with
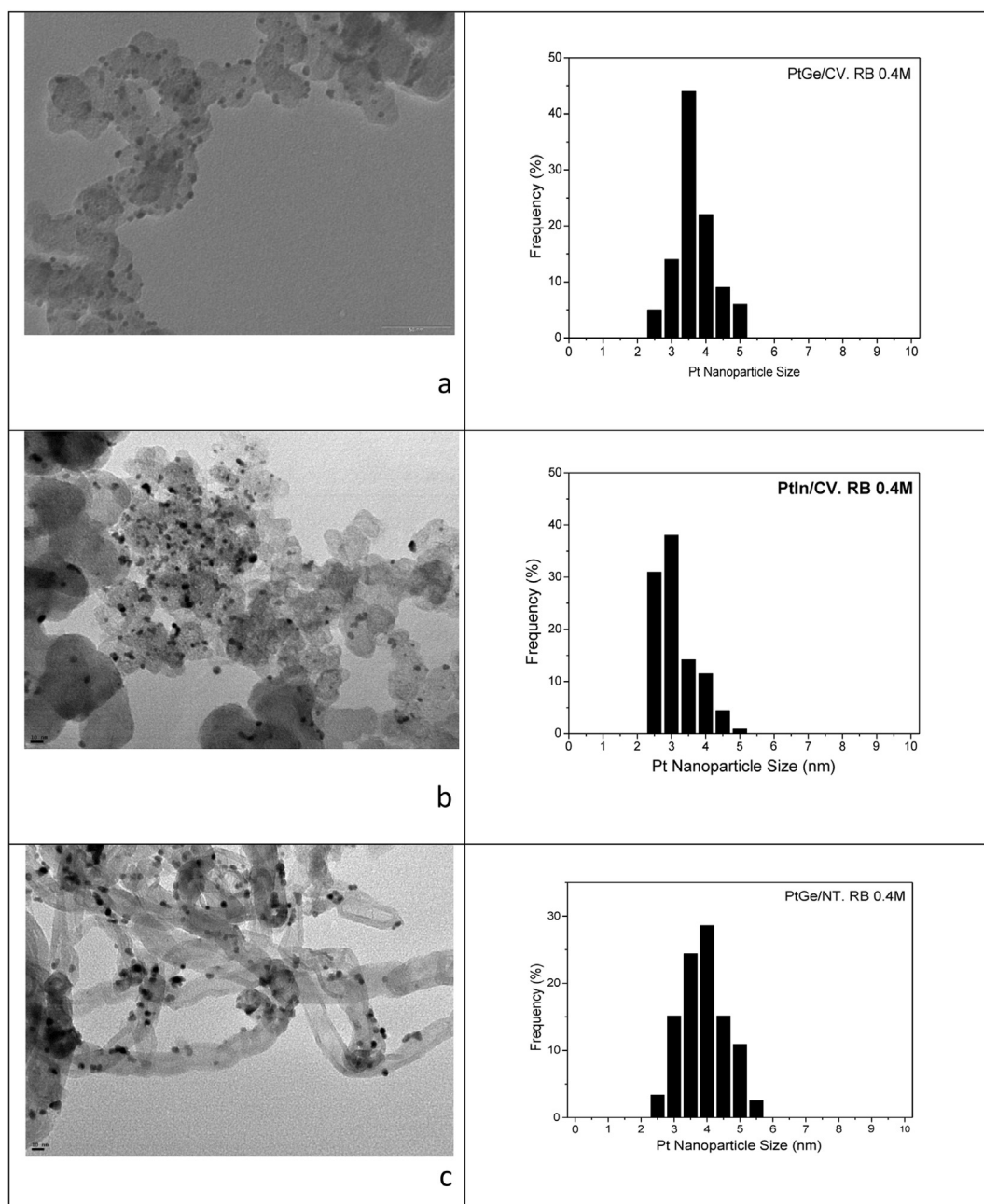

Fig. 6 – TEM images corresponding to: a) PtGe/CV, b) PtIn/CV, c) PtGe/NT, together with their corresponding size distribution histograms.

supported Pt and PtGe catalysts. It can be observed that for PtGe catalysts supported on CV and NT, the polarization curves (70 °C and P = 1 atm) are similar to that of the commercial catalyst, although there is a shift of the maximum power to lower current densities (Fig. 4a)). In these conditions (70 °C and 1 atm at the cathode), the incidence of crossover of methanol is important, hence experiments at higher pressures at the cathode demonstrated the inhibition of this effect. In this sense, at 90 °C and 2 atm at the cathode, the performance of PtGe/VC y PtGe/NT is clearly enhanced both in the power and in the polarization curve, giving a maximum of the power density equal to 70 mW/cm^2 at a current density of 450 mA/cm^2 (Fig. 4b)). Besides, Fig. 5a) and b) shows the polarization and power density curves obtained in DMFC with supported Pt and PtIn catalysts. In the case of PtIn catalysts supported on CV and NT (Fig. 5a)) (at 70 °C and 1 atm), a smaller power density with respect to the commercial catalyst is observed, while at 90 °C and 2 atm, PtIn/CV shows a power density slightly higher than the commercial catalyst (see Fig. 5b)). On the other hand, PtIn/NT does not display a good behaviour at 90 °C and 2 atm. With respect to the bimetallic catalysts supported on MC, they do not show a good performance not only with respect to the commercial catalyst, but also with respect to PtGe and PtIn catalysts supported on CV and NT. From these results it can be inferred not only the important role of the support but also the better behaviour of the catalysts supported on CV, followed by those supported on NT.

Finally, PtGe/CV, PtIn/VC and PtGe/NT catalysts, which displayed the best performance in activity for DMFC, were characterized by Transmission Electronic Microscopy (TEM) in order to determine the distribution of metallic particles over each carbonaceous support.

It must be taken into account that the distribution of metallic particles of both monometallic Pt catalysts supported on carbon Vulcan and carbon nanotubes showed a wide distribution of Pt particles from 3 to 10 nm, with mean particle sizes of 6 and 5 nm, respectively. These TEM results were previously published [16].

The TEM images corresponding to the three bimetallic catalysts, PtGe and PtIn supported on carbon Vulcan, and PtGe supported on nanotubes, together with their corresponding size distribution histograms, are shown in Fig. 6a), b) and c)). These bimetallic catalysts show a more homogeneous and narrower distribution of particle sizes than the corresponding Pt catalysts. The mean diameters of the particles of PtGe/CV, PtIn/CV and PtGe/NT catalysts are 3.5, 3 and 3.7 nm, respectively, and all catalysts display a narrow distribution of metallic particles from 2 to 5 nm. These results are in agreement with the increase of the amounts of chemisorbed hydrogen found for bimetallic catalysts with respect to those of the corresponding monometallic ones.

This means that the presence of both promoters (Ge or In) during the deposition–reduction technique of the samples produce a decrease of the particle sizes (determined by chemisorptions, XRD and TEM) and a narrower distribution (determined by TEM), with respect to the corresponding monometallic ones. Hence there is an increase of the metallic dispersion of these bimetallic catalysts with the consequent increment of the electrocatalytic activity in DMFC.

The deposition–reduction in liquid phase with sodium borohydride of PtGe and PtIn supported on carbon Vulcan and carbon nanotubes leads to a metallic phase with a narrower distribution (2–5 nm) with respect to Pt catalysts, which indicates that Ge or In favour the dispersion of the catalyst. Besides, taking into account that from characterization techniques mainly geometric effects were found, the presence of Ge or In in the surroundings of the new and small particles, probably by a decoration effect of Ge or In around Pt, would produce important promoter effects both for an easier CO oxidation to CO$_2$ (observed in CO stripping experiments) and for a higher electrocatalytic activity (determined in DMFC experiments).

4. Conclusions

- The deposition–reduction method in liquid phase (with sodium borohydride) of bimetallic PtGe and PtIn catalysts leads to a good reducibility of platinum. However Ge species remain as oxidized ones, while there is a partial reduction of In species.

- Results of H$_2$ chemisorption and test reaction of the metallic phase (benzene hydrogenation) indicate low electronic interactions between Pt and the second metal, Ge or In, However the presence of geometric effects, related with a probable decoration of Ge or In around the small Pt particles, appears to be important.

- There is an important role of the support type on the characteristics of the deposited metallic phase and on the electrochemical behaviour of the electrocatalysts. The best electrocatalytic performance was obtained by using carbon Vulcan as support of bimetallic catalysts, followed by carbon nanotubes. On the other hand the performance of mesoporous carbon as support was not adequate.

- The presence of Ge or In in the surroundings of small Pt particles produces important promoter effects both for an easier CO oxidation to CO$_2$ (observed in CO stripping measurements) and for a higher electrocatalytic activity (determined in DMFC experiments).

REFERENCES

[1] Iwasita T. Handbook of fuel cells, vol. 2. Chichester, UK: Wiley; 2003.

[2] Müller J, Frank G, Colbow K, Wilkinson D. Handbook of fuel cells, vol. 4. Chichester, UK: Wiley; 2003.

[3] Hamnett A. Mechanism and electrocatalysis in the direct methanol fuel cell. Catal Today 1997;38:445–57.

[4] Batista EA, Malpass GRP, Motheo AJ, Iwasita T. New mechanistic aspects of methanol oxidation. J Electroanal Chem 2004;571:273–82.

[5] Aricó AS, Srinivasan S, Antonucci V. DMFCs: from fundamental aspects to technology development. Fuel Cell 2001;1:133–61.

[6] Ehteshamia SMM, Chana SH. A review of electrocatalysts with enhanced CO tolerance and stability for polymer electrolyte membrane fuel cells. Electrochim Acta 2013;93:334–45.

[7] Man-Yin L, I-Husan L, Chun-Chieh H. Key issues in the preparation of DMFC electrocatalysts. Int J Hydrogen Energy 2007;32:731–5.

[8] Vielstich W. Fuel cells technology and applications, vol. 3. Chichester, UK: Wiley; 2003.

[9] Antolini E. Platinum alloys as anode catalysts for direct methanol fuel cells. In: Liu H, Zhang J, editors. Electrocatalysis of direct methanol fuel cells: from fundamentals to applications. Weinheim, Germany: Wiley-VCH Verlag GmbH & Co.; 2009. pp. 227–55.

[10] Dubau L, Hahn F, Coutanceau C, Léger JM, Lamy C. On the structure effects of bimetallic PtRu electrocatalysts towards methanol oxidation. J Electroanal Chem 2003;554–555:407–15.

[11] Neto AO, Dias RR, Tusi MM, Linardi M, Spinacé EV. Electro-oxidation of methanol and ethanol using PtRu/C, PtSn/C and PtSnRu/C electrocatalysts prepared by an alcohol-reduction process. J Power Sources 2007;166:87–91.

[12] Crabb EM, Ravikumar MK. Synthesis and characterisation of carbon-supported PtGe electrocatalysts for CO oxidation. Electrochim Acta 2001;46:1033–41.

[13] Chu D, Li Z, Yuan X, Li J, Wei X, Wan Y. Electrocatalytic properties of carbon nanotubes supported ternary PtSnIn catalysts for ethanol electro-oxidation. Electrochim Acta 2012;78:644–8.

[14] Bruno MM, Cotella NG, Miras MC, Barbero C. A novel way to maintain resorcinol-formaldehyde porosity during drying: stabilization of the sol gel nanostructure using a cationic polyelectrolyte. Colloids Surf A 2010;362:28–32.

[15] Bruno MM, Corti HR, Balach J, Cotella GN, Barbero CA. Hierarchical porous materials: capillaries in nanoporous carbon. Funct Mater Lett 2009;2:135–8.

[16] Veizaga N, Fernandez J, Bruno M, Scelza O, de Miguel S. Deposition of Pt nanoparticles on different carbonaceous materials by using different preparation methods for PEMFC electrocatalysts. Int J Hydrogen Energy 2012;37:17910–20.

[17] Benson JE, Boudart M. Hydrogen-oxygen titration method for the measurement of supported platinum surface areas. J Catal 1965;4:704–71.

[18] Maillard F, Eikerling M, Cherstiouk OV, Schreier S, Savinova E, Stimming U. Size effects on reactivity of Pt nanoparticles in CO monolayer oxidation: the role of surface mobility. Faraday Discuss 2004;125:357–77.

[19] de Miguel SR, Vilella JI, Jablonski EL, Scelza OA, Salinas-Martinez de Lecea C, Linares-Solano A. Preparation of Pt catalysts supported on activated carbon felts (ACF). Appl Catal A Gen 2002;232:237–46.

[20] Wagner CD, Riggs WM, Davis LE, Moulder JF, Muilenberg GE. Handbook of X-ray photoelectron spectroscopy. Perkin Elmer Co., Physical Electronics; 1979.

[21] Patterson AL. The Scherrer formula for X-Ray particle size determination. Phys Rev 1939;56:978–82.

[22] Poondi D, Vannice MA. Competitive hydrogenation of benzene and toluene on palladium and platinum catalysts 1996;751:742–51.

[23] Haller G. New catalytic concepts from new materials: understanding catalysis from a fundamental perspective, past, present, and future. J Catal 2003;216:12–22.

[24] Vidakovic T, Christov M, Sundamcher K. The use of CO stripping for in situ fuel cell catalyst characterization. Electrochim Acta 2007;52:5606–13.

[25] Vengatesan S, Kim HJ, Kim SK, Oh IH, Lee SY, Cho EA, et al. High dispersion platinum catalyst using mesoporous carbon support for fuel cell. Electrochim Acta 2008;54:856–61.